Systematic underestimation of earthquake magnitudes from large intracontinental reverse faults: Historical ruptures break across segment boundaries

C. M. Rubin
Department of Geology, Central Washington University, Ellensburg, Washington 98926,
and Southern California Earthquake Center, Los Angeles, California 90089

ABSTRACT

Because most large-magnitude earthquakes along reverse faults have such irregular and complicated rupture patterns, reverse-fault segments defined on the basis of geometry alone may not be very useful for estimating sizes of future seismic sources. Most modern large ruptures of historical earthquakes generated by intracontinental reverse faults have involved geometrically complex rupture patterns. Ruptures across surficial discontinuities and complexities such as stepovers and cross-faults are common. Specifically, segment boundaries defined on the basis of discontinuities in surficial fault traces, pronounced changes in the geomorphology along strike, or the intersection of active faults commonly have not proven to be major impediments to rupture. Assuming that the seismic rupture will initiate and terminate at adjacent major geometric irregularities will commonly lead to underestimation of magnitudes of future large earthquakes.

INTRODUCTION

The potential for earthquakes along intracontinental reverse faults has been dramatically illustrated by several recent earthquakes. Examples include the destructive earthquakes in 1971, 1980, 1987, and 1994 in California, Algeria, and Armenia (Kamb et al., 1971; Philip and Meghraoui, 1983; Philip et al., 1992; Hauksson et al., 1994). These earthquakes have sparked fundamental questions about the potential size of an earthquake generated along reverse faults in continental settings at a time when the use of fault segmentation models for the evaluation of seismic hazards has been popular. In this paper, fault segment boundaries are defined as discontinuities in surficial fault trace (e.g., stepovers or gaps), changes in fault orientation, pronounced changes in the geomorphology along strike, or the intersection with active faults or folds that may potentially act as barriers to earthquake ruptures. Some models also include along-strike variations in slip rate and creeping vs. locked behavior, which may or may not coincide with geometric discontinuities. Although the application of characteristic earthquake models that use fault-segment length in earthquake size predication is under considerable debate, earthquake hazard analyses typically use rupture length and recurrence rate for calculating earthquake hazard probabilities (e.g., Wesnousky, 1986; Working Group on California Earthquake Probabilities, 1995). Because the size of an expected earthquake is primarily controlled by rupture length, a greater fault rupture length will result in a larger magnitude earthquake. Identifying segment boundaries of faults that will be the source of future earthquakes is critical in hazard analyses. If many segments along a fault break simultaneously, the expected earthquake will be considerably greater than if rupture occurs along individual segments.

In some well-understood strike-slip settings, such as along the Imperial Valley and Superstition faults in California, segmentation models have been useful for evaluating seismic hazards. For example, surface rupture occurred along the entire known 60 km length of the Imperial fault during the 1940 El Centro earthquake (M = 7.1) (Buwalda and Richter, 1941; Ulrich, 1941), whereas during the M = 6.6 earthquake of 1979, slip occurred only along the northern half of the surface trace of the Imperial fault (Sharp et al., 1982). Although dextral surface offsets in 1940 were as great as 6 m, offsets along the northern part of the fault were roughly comparable to those of 1979, ~10–20 cm (Sieh, 1996). Thus it appears that the steep northward decrease in slip during the 1940 El Centro earthquake coincides with the steep southward decrease documented after the 1979 Imperial earthquake. The similarities of these two earthquakes suggest that the Imperial fault may consist of discrete segments, each of which has a characteristic magnitude of slip through several earthquake cycles. In contrast to these successful applications of fault segmentation models, surface rupture occurred across multiple segments along several discrete faults traces during the 1992 Landers strike-slip earthquake (Sieh et al., 1993). The involvement of several discrete faults in a single earthquake complicates the use of fault-segment length models in the prediction of the size of future earthquakes.

Using geologic slip rates and moment magnitude relations, Dolan et al. (1995) proposed that reverse faults within the Los Angeles region are capable of producing large earthquakes in the range of M_w 7.2 to 7.6 along multiple fault segments. Dolan et al. (1995) concluded that in order to satisfy moment-rate calculations and the historical record, reverse faults in southern California probably break across geometric boundaries. The best test of the use of geometric segments is the historical record that consists of seven moderate to large (M = 6.5 to 8), globally distributed events from the 1896 Riku-u, 1932 Chang Ma, 1980 El Asnam, 1952 White Wolf, 1971 San Fernando, and 1988 Spitak earthquakes (Fig. 1). Although there are other historical seismogenic intracontinental reverse faults (e.g., 1906 Manas, 1911 Chon-Kemin, and the 1914 Balikan He earthquakes in central Asia), only those earthquakes that have well-documented surface rupture are included in this compilation. In light of the potential for large-magnitude earthquakes along intracontinental reverse faults, this study explores the application of fault segmentation models to reverse faults and the resulting systematic underestimation of potential earthquake magnitude.

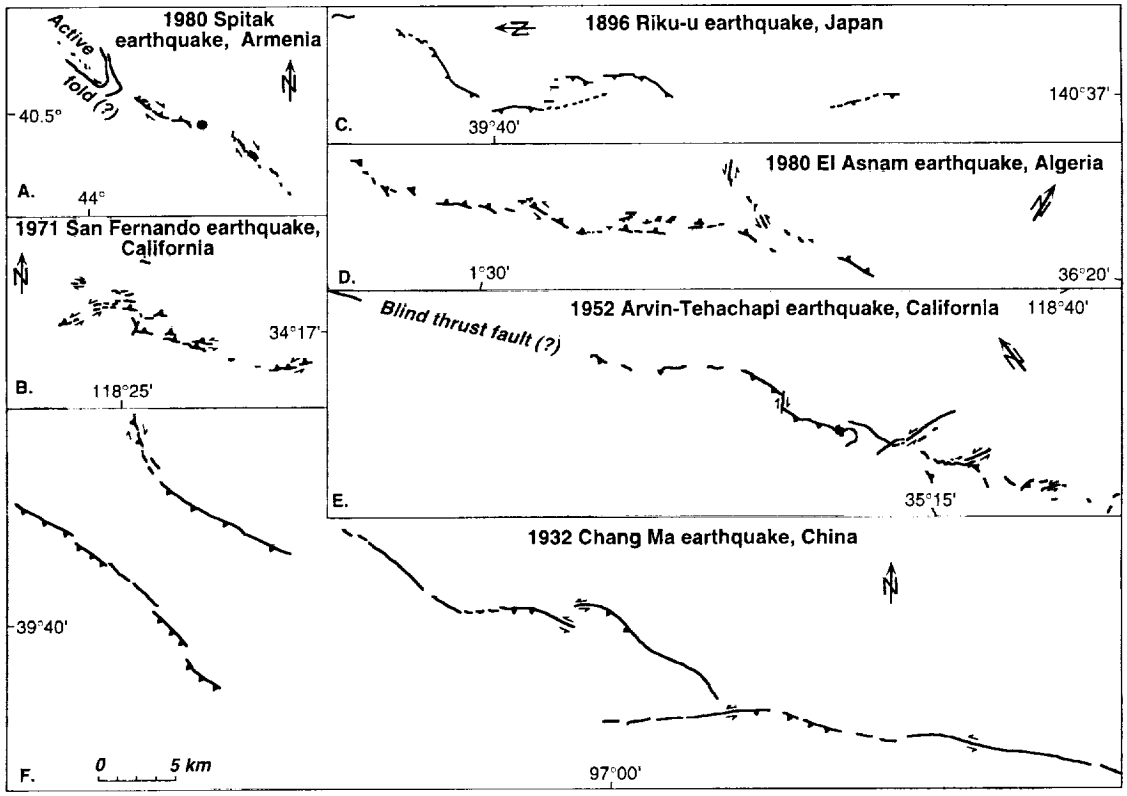

Figure 1. Global compilation of historical surface rupture along large magnitude intracontinental reverse faults. Scale applies to all insets. A: 1988 Spitak earthquake after Philip et al. (1992). B: 1971 San Fernando earthquake after Kamb et al. (1971). C: 1896 Riku-u earthquake after Matsuda et al. (1980). D: 1980 El Asnam earthquake after Philip and Meghraui (1983). E: 1952 Arvin-Tehachapi earthquake after Buwalda and St. Amand (1955). F: 1932 Chang Ma earthquake after Meyer (1991).

HISTORICAL RUPTURES

1896 Riku-u Earthquake

The 1896 Riku-u earthquake (M ≈ 7.5) occurred in the Tohoku district of northeastern Japan. Surficial rupture occurred on four main segments. The maximum vertical displacement was about 350 cm, and no strike-slip component was observed (Matsuda et al., 1980) (Fig. 1). The three central segments that make up most of the surface rupture total 20.5 km in length and consist of three discontinuous reverse faults that vary considerably in strike, from N30°E to north-south (Fig. 1). Separation of each of the three central main segments is 1 and 5 km. The northernmost segment is 5.5 km long and is separated by more than 9 km from the other three segments (Fig. 1). Offset along all four fault segments is east-side up, and the total rupture length is about 36 km. A fifth segment ruptured about 15 km to the east of the three central main segments (Matsuda et al., 1980) (Fig. 1). The maximum vertical offset was about 2 m (Matsuda et al., 1980). Unlike the four western segments, the eastern segment shows west-side-up displacement and is 6 km long. The eastern segment strikes N45°E, in contrast to the more northerly strike of the other four segments. The rupture pattern was made even more complex by the failure of conjugate reverse faults that dip toward the main traces.

1932 Chang Ma Earthquake

The 1932 Chang Ma earthquake (M ≈ 7.6) occurred in northern China and involved five separate major fault segments (Meyer, 1991). Four of the segments are thrust faults; the fifth segment is a strike-slip fault (Meyer, 1991; Peltzer et al., 1988). The total length of all reverse ruptures is about 115 km; stepovers between segments are 2–10 km. The first segment, located to the southwest, is 35 km long. Rupture is discontinuous, and there are vertical offsets of about 50 cm (Meyer, 1991) (Fig. 1). The second segment, located about 10 km to the northeast, is 29 km long and consists of a series of discontinuous surface ruptures. Vertical offsets are about 2 m. A third segment, located about 4 km farther east, is arcuate in shape, and has vertical displacements of 1.5 m and sinistral displacements of about 1.5 m. Strike varies considerably along the length of this segment. A fourth segment, located a few kilometres farther to the northeast, is 23.5 km long and consists of discontinuous oblique reverse, strike-slip, and normal surface ruptures. The surficial width of the rupture zone is more than 0.5 km. The maximum vertical offset was 5 m.

1952 Arvin-Tehachapi Earthquake

The Arvin-Tehachapi earthquake (M ≈ 7.7), which occurred in southern California, was produced by the White Wolf fault and involved rupture of four principal faults (Buwalda and St. Amand, 1955). The principal surface rupture consists mainly of oblique-reverse slip displacement; there is a maximum of 120 cm of vertical offset and 60 cm of dextral strike-slip offset (Buwalda and Richter, 1941). The easternmost segment consists of discontinuous oblique reverse and short, discontinuous sinistral strike-slip faults; this segment is ~12 km long (Fig. 1). To the west, another fault segment is separated from the eastern segment by a north-trending sinistral strike-slip fault and is 4.5 km long (Fig. 1). In both of these segments, the strike of surface rupture changes from north-south to east-west. The central segment is about 12 km long and consists of a series of arcuate oblique reverse faults and reverse faults (Fig. 1). A north-trending oblique reverse fault bounds the central segment on the east. Farther westward, a discontinuous surface rupture is present for more than 7 km. The main zone of surface rupture is ~22 km from the westernmost segment. A northwest-trending, 3-km-long surface rupture marks the western extent of surface faulting. Although the total strike length of the surface rupture was 43 km, no surface rupture was observed for more than 22 km between the westernmost rupture and the main zone of surface rupture. This interpretation agrees with the seismic and

geodetic data from the earthquake (Richter, 1955; Stein and Thatcher, 1981).

1971 San Fernando Earthquake

The surface rupture of the 1971 San Fernando earthquake (M = 6.6) occurred on the southern flank of the San Gabriel Mountains and along the northern portion of the San Fernando Valley in southern California. The fault ruptured in five segments, all of which involved slip along thrust and minor strike-slip faults. The westernmost segment (Mission Wells segment) is about 2 km long and consists of minor sinistral strike-slip and reverse surface faulting. The second segment (Sylmar segment) is 2.5 km eastward. This segment is 3 km long, strikes east-west, and has a maximum vertical offset of 30 cm and sinistral strike-slip offset of 100 cm (Kamb et al., 1971). A 1-km-long complex rupture zone transfers slip between the Sylmar and the third, Tujunga, segment. The Tujunga segment discontinuously ruptured along the southern edge of the San Gabriel foothills for more than 7 km (Fig. 1). Vertical slip and sinistral slip at the surface vary considerably along strike; vertical slip is ~1 m and sinistral offsets are >1 m. Series of minor reverse and dextral-slip faults are ~0.3–0.9 km north of the main faults of the Tujunga segment. Minor surface rupture along a reverse fault is located about 2.5 km north of the Sylmar segment. All segments have an approximately east-west strike and vary in both thrust and strike-slip offsets. The total rupture length is about 20 km. On the basis of teleseismic long-period body waves, Heaton (1982) concluded that the earthquake was produced by two distinct sources along two separate faults. Initial rupture occurred at a depth of ~15 km to a depth of 3 km. Vertical uplift and strong-motion data suggest that the majority of faulting on the Sierra Madre fault occurred at depths between 3 and 16 km (Heaton, 1982). A second, larger event initiated ~4 s later at a depth of 8 km and propagated to the surface. Teleseismic body-wave modeling indicates that much of the slip occurred at depths >3 km. This interpretation is consistent with the fact that the up-dip projection of the focal mechanism does not coincide with the observed surface rupture. Thus, slip generated from the first source produced rupture along the Sierra Madre fault at depth, and the second source produced slip on the San Fernando fault. Slip along two separate, subparallel thrust faults at depth resulted in a complex rupture mechanism at depth and on the surface.

1980 El Asnam Earthquake

The 1980 El Asnam earthquake (M = 7.3) was the largest earthquake of the twentieth century in the Tellian Atlas Mountains of Algeria, North Africa. The rupture pattern is complex; thrust, normal, and strike-slip faults and tensile fractures are present along much of the surface trace (Philip and Meghraoui, 1983) (Fig. 1). The rupture occurred along five segments (Fig. 1); the main four segments are about 40 km long. The width of the surface trace varies from a few metres to more than 1 km. The segments are not linear and vary in strike from N40°–45°E to N70°–80°E. In the southernmost first segment, surface breaks are confined to a narrow zone of discontinuous reverse faults; there is minor sinistral strike-slip offset. The second segment to the northeast displays discontinuous reverse slip; the maximum vertical offset is 500 cm. Normal faults were observed from 500 m to more than 1.5 km laterally away from the main zone of reverse faults. To the north, the third segment consists of a series of reverse-slip faults and an elongate zone of en echelon grabens that are oblique to the main reverse fault. The northernmost, fourth segment differs in orientation from the other segments exposed to the south. There, the surface trace strikes N80°E, whereas to the south, the average strike of the surface rupture is about N40°–45°E. The rupture pattern is also very complicated in the northern segment; there are vertical offsets between 15 and 40 cm on small, discontinuous short faults. Farther to the north, these discontinuous faults form a single fault trace, that has vertical displacements of as much as 500 cm. The fifth main segment displays an arcuate pattern, and a discontinuous reverse fault that strikes from east-west to N70°W. A maximum vertical offset of 200 cm was observed (Philip and Meghraoui, 1983).

1988 Spitak Earthquake

The 1988 Spitak earthquake (M = 7.0) occurred in northern Armenia and is characterized by complex fault segmentation. It involved both surface faulting and folding associated with a blind thrust (Philip et al., 1992). The rupture is composed of four separate segments, three of which reach the surface. The southeastern segment has a rupture length of about 11 km and consists of a right-lateral en echelon system of strike-slip faults; the maximum offset is about 50 cm (Philip et al., 1992) (Fig. 1). Ruptures are very discontinuous. A complicated and discontinuous rupture pattern with reverse, dextral and sinistral strike-slip, and normal fault offsets, is observed along the central segment (Fig. 1). Horizontal displacement increases to the west; there is a maximum vertical offset of 160 cm and a corresponding 40 cm of dextral offset. The maximum dextral offset is about 100 cm. A discontinuous rupture pattern is observed along the central segment (Fig. 1), and there are reverse, dextral and sinistral strike-slip, and normal fault offsets. In addition, en echelon folds, extensional fractures, and tear faults characterize portions of the central segment. The third and fourth segments are located to the northwest of the central segment (Fig. 1) and consist of short, discontinuous, 200-m-long reverse fault ruptures, that have 8 cm of vertical offset; tension fractures and large landslides are also present. A blind thrust fault may be present at depth, because the reverse fault broke along a hinge of an anticline. Aftershock distribution and focal mechanisms support this interpretation (Dorbath et al., 1992). The total length of fault rupture and folding is about 40 km and corresponds to a seismic moment of 0.3×10^{20} Nm (Haessler et al., 1992). The analysis of teleseismic waves of Kikuchi et al. (1993) shows a multiple source mechanism for the earthquake. Subevents 1 and 2 occurred during the first 20 s. A large secondary dip-slip event occurred ~30 s after the initial rupture. This event had a slower moment release rate and involved ~40% of the total moment.

DISCUSSION

The historical earthquake rupture patterns of large magnitude earthquakes on intracontinental reverse faults show that multiple ruptures across segment boundaries are common. For example, in the 1932 Chang Ma earthquake, at least five separate fault segments ruptured. The 1896 Riku-u earthquake involved three main segments that differ in strike and two additional segments that are separated by 5 to 15 km from the main segments. These are typical of several large reverse faults that display complex rupture and geomorphic patterns. Discontinuous zones of rupture span 100 m to more than 3.5 km in width. The surface trend and magnitude of displacement also vary widely along strike. Gaps as long as 5 km between stepovers are common. In addition, ruptures occur along numerous long, oblique, intersecting faults. Thus the determination of "geologically reasonable" segment lengths for reverse faults, which ultimately control the size of an earthquake, is more complex than current models assume (Allen, 1968; Schwartz and Sibson, 1989). Rupture at depth also appears to be complex. Studies of teleseismic body waves for the 1971 San Fernando and 1988 Spitak earthquakes by Heaton (1982) and Kikuchi et al. (1993) sug-

gest that dip-slip events exhibit complex waveforms that involve multiple source mechanisms. The results are consistent with the observed highly variable surface rupture patterns. The existence of a slow after-slip event with a mechanism different from the two initial events during the 1988 Spitak earthquake may have also played a role in the observed complex pattern of surface deformation. The four subevents identified by Kikuchi et al. (1993) for the 1988 Spitak earthquake correlate remarkably well with the observed variations in surface rupture, where the slow subevent probably occurred in the area characterized by active folding. Perhaps large reverse fault events that are characterized by multiple surface ruptures indicate complex source mechanisms.

Because most large-magnitude earthquakes along reverse faults have complicated rupture patterns, reverse fault segments that can be readily identified on a geometric or structural basis do not always represent mechanically independent seismic sources. For this reason, segment boundaries defined on the basis of pronounced separations or gaps in surface fault traces, changes in fault orientation or stepovers, pronounced changes in the geomorphology along strike, the intersection of active faults and folds, or termination at cross-structure discontinuities do not necessarily arrest rupture propagation, nor do they limit the size of earthquakes on reverse faults. Well-documented historical ruptures that break across several such segments indicate that segmentation models systematically underestimate the maximum magnitude of earthquakes on intracontinental reverse faults.

CONCLUSIONS

Large intracontinental reverse faults are globally distributed and pose hazards to densely populated areas. Although fault segmentation models are commonly used to estimate seismic risk, these models assume that simple segmentation controls earthquake magnitude. Historic ruptures of large earthquakes on intracontinental reverse faults show that simple segmentation is not characteristic. Instead, large earthquakes rupture multiple segments in single earthquakes. Thus seismic risk along intracontinental reverse faults has been systematically underestimated. The potential magnitude of an earthquake along such a fault is far greater if numerous segments break simultaneously.

ACKNOWLEDGMENTS

During the initial stages of this study, I was partially supported by the Seismological Laboratory at the California Institute of Technology. This research was supported by National Aeronautics and Space Administration grant NAGW-3691 and the Southern California Earthquake Center/National Science Foundation grant EAR-8920136. Kerry Sieh and Peter Molnar suggested many improvements in the manuscript and provided encouragement. Joann Stock and Martitia Tuttle provided constructive reviews. Southern California Earthquake Center contribution 338.

REFERENCES CITED

Allen, C. R., 1968, The tectonic environments of seismically active and inactive areas along the San Andreas fault system, *in* Proceedings of the Conference on Geologic Problems of the San Andreas Fault System: Stanford University Publications, Geological Sciences, v. 11, p. 70–82.

Buwalda, J. P., and Richter, C., 1941, Imperial Valley earthquake of May 18, 1940 [abs.]: Geological Society of America Bulletin, v. 52, p. 1944–1945.

Buwalda, J. P., and St. Amand, P., 1955, Geological effects of the Arvin-Tehachapi earthquake, California, *in* Earthquakes in Kern County California during 1952: California Division of Mines and Geology Bulletin, v. 171, p. 51–56.

Dolan, J. F., Sieh, K., Rockwell, T. K., Yeats, R. S., Shaw, J., Suppe, J., Huftile, G. J., and Gath, E. M., 1995, Prospects for larger or more frequent earthquakes in the Los Angeles metropolitan region: Science, v. 267, p. 199–205.

Dorbath, L., Dorbath, C., Rivera, L., Fuenzalida, A., Cisternas, A., Tatevossian, R., Aptekman, J., and Arefiev, S., 1992, Geometry, segmentation and stress regime of the Spitak (Armenia) earthquake from analysis of the aftershock sequence: Geophysical Journal International, v. 108, p. 309–328.

Haessler, H., Deschamps, A., Dufumnier, H., Fuenzalida, H., and Cisternas, A., 1992, The rupture process of the Armenian earthquake from broad-band teleseismic body wave records: Geophysical Journal International, v. 109, p. 151–161.

Hauksson, E., Hutton, K., Kanamori, H., Jones, L., and Mori, J., 1994, The M_w 6.7 Northridge, California, earthquake of January 17, 1994 and its aftershocks: Seismological Society of America, Annual Meeting, 89th Program for Northridge Abstracts, Abstract 1.

Heaton, T. H., 1982, The 1971 San Fernando earthquake: A double event?: Seismological Society of America Bulletin, v. 72, p. 2037–2062.

Kamb, B., Silver, L. T., Abrams, M. J., Carter, B. A., Jordan, T. H., and Minster, J. B., 1971, Pattern of faulting and nature of fault movement in the San Fernando earthquake, *in* The San Fernando, California, 1971: Pattern of faulting and nature of fault movement in the San Fernando earthquake: U.S. Geological Survey Professional Paper 773, p. 41–54.

Kikuckhi, M., Kanamori, H., and Satake, H. K., 1993, Source complexity of the 1988 Armenian earthquake: Evidence for a slow after-slip event: Journal of Geophysical Research, v. 98, p. 15797–15808.

Matsuda, T., Yamazaki, H., Nakata, H., and Imaizumi, T., 1980, The surface faults associated with the Riku-u earthquake of 1986: Bulletin of the Earthquake Research Institute, Tokyo University, v. 55, p. 795–855 (in Japanese).

Meyer, B., 1991, Méceanismes des Grands Tremblements de Terre et du Raccourcissement Crustal Oblique au Bord Nord-est du Tibet [thesis]: Paris, Université Paris, 129 p.

Peltzer, G., Tapponnier, P., Gaudemer, Y., Meyer, B., Guo Shunmin, Yin Kelun, Chen Zhitai, and Dai Huagung, 1988, Offsets of late Quaternary morphology, slip rate, and recurrence of large earthquakes on the Chang Ma fault (Gansu, China): Journal of Geophysical Research, v. 93, p. 7793–7812.

Philip, H., and Meghraoui, M., 1983, Structural analysis and interpretation of the surface deformations of the El Asnam earthquake of October 10, 1980: Tectonics, v. 2, p. 17–49.

Philip, H., Rogozhin, E., Cisternas, A., Bousquet, J. C., Borisov, B., and Karakhanian, A., 1992, The Armenian earthquake of 1988 December 7: Faulting and folding, neotectonics and palaeoseismicity: Geophysical Journal International, v. 110, p. 141–158.

Richter, C. F., 1955, Foreshocks and aftershocks, *in* Earthquakes in Kern County California during 1952: California Division of Mines and Geology Bulletin, v. 171, p. 177–198.

Schwartz, D. P., and Sibson, R. H., 1989, Introduction to workshop on fault segmentation and controls of rupture initiation and termination, *in* Fault segmentation and controls of rupture initiation and termination: U.S. Geological Survey Open-File Report 89-314.

Sharp, R., and 15 others, 1982, Surface faulting in the central Imperial Valley, the Imperial Valley, California, earthquake of October 15, 1979: U.S. Geological Survey Professional Paper, 1254, p. 119–143.

Sieh, K., 1996, The repetition of large-earthquake ruptures: National Academy of Sciences Proceedings, v. 93, p. 3764–3771.

Sieh, K., and 19 others, 1993, Near-field investigations of the Landers earthquake sequence, April to July 1992: Science, v. 260, p. 171–176.

Stein, R. S., and Thatcher, W., 1981, Seismic and aseismic deformation associated with the 1952 Kern County, California, earthquake and relationship to the Quaternary history of the White Wolf fault: Journal of Geophysical Research, v. 86, p. 4913–4928.

Ulrich, F., 1941, The Imperial Valley earthquake of 1940: Seismological Society of America Bulletin, v. 31, p. 13–31.

Wesnousky, S. G., 1986, Earthquakes, Quaternary faults, and seismic hazards in California: Journal of Geophysical Research, v. 91, p. 12587–12631.

Working Group on California Earthquake Probabilities, 1995, Seismic hazards in southern California: Probable earthquakes, 1994 to 2024: Seismological Society of America Bulletin, v. 85, p. 379–439.

Manuscript received March 27, 1996
Revised manuscript received July 15, 1996
Manuscript accepted August 19, 1996